Biology of Reproduction, 2017, 96(6), 1210–1220
doi:10.1093/biolre/iox052
Research Article
Advance Access Publication Date: 1 June 2017

Research Article

Changes in immune cell distribution and their cytokine/chemokine production during regression of the rhesus macaque corpus luteum†

Cecily V. Bishop[1,*], Fuhua Xu[1], Rosemary Steinbach[1], Ellie Ficco[1], Jeffrey Hyzer[1], Steven Blue[2], Richard L. Stouffer[1,3] and Jon D. Hennebold[1,3]

[1]Division of Reproductive and Developmental Sciences, Oregon National Primate Research Center, Oregon, USA; [2]Endocrine Technology Support Core Laboratory, Oregon National Primate Research Center, Beaverton, Oregon, USA and [3]Department of Obstetrics and Gynecology, Oregon Health and Science University, Portland, Oregon, USA

*Correspondence: Division of Reproductive and Developmental Sciences, Oregon National Primate Research Center, 505 NW 185th Ave, Beaverton, OR 97006, USA. E-mail: bishopc@ohsu.edu

†**Grant Support:** The work is supported in part by R01HD020869 (RLS, JDH) and P51OD011092 (Support for Primate Research Center, PI: Robertson, J. E.).
Conference Presentation: These data were presented, in part, at the 47th Annual Meeting of the Society for the Study of Reproduction, July 2014.

Received 19 December 2016; Revised 16 May 2017; Accepted 30 May 2017

Abstract

Our previous flow cytometry results demonstrated a significant increase in neutrophils, macrophages/monocytes, and natural killer (NK) cells in dispersed rhesus monkey corpora lutea (CL) after progesterone (P4) levels had fallen below 0.3 ng/ml for ≥3 days during the natural menstrual cycle. In this study, immunohistochemistry revealed the $CD11b^+$ cells (neutrophils, macrophages/monocytes) present in the CL after luteal P4 synthesis ceased were distributed throughout the tissue. $CD16^+$ cells (presumptive NK cells) were observed mainly near the vasculature in functional CL, until their numbers increased and they became widely distributed in regressing CL. To determine if the immune cells that enter luteal tissue during structural regression are functionally different from those that are present during peak function, $CD11b^+$ or $CD16^+$ populations were enriched from mid-late stage (functional) and regressing (days 1.8 ± 0.3 postmenses) CL using antibody-conjugated magnetic microbeads. Flow cytometry analyses revealed the majority of $CD11b^+$ cells expressed CD14, a protein mainly produced by macrophages/monocytes. The antibody-enriched and depleted fractions were cultured for 24 h, and the media then analyzed for the production of 29 cytokines/chemokines. From the mid-late CL, the $CD11b^+$-enriched fraction produced three cytokines/chemokines, whereas $CD16^+$-enriched cells only produced the chemokine CCL2. However, $CD11b^+$-enriched cells isolated from regressed CL produced eight cytokines/chemokines. The $CD16^+$-enriched cells isolated from regressing CL produced significant levels of only three cytokines. Thus, the $CD11b^+$ cells that appear in the rhesus macaque CL after functional regression produce several cytokines/chemokines that likely play a role in orchestrating structural regression.

Summary Sentence

Cessation of progesterone synthesis at the end of the menstrual cycle leads to increases in monocytes/macrophage and neutrophil numbers, as well as in the type and level of the chemokines and cytokines they secrete.

Key words: corpus luteum, macrophage, neutrophil, natural killer cell, chemokine, cytokine.

Introduction

The primate corpus luteum (CL) is a transient endocrine gland that forms from the cell populations originally comprising the wall of the ovulatory follicle; these include steroidogenic/secretory, vascular/lymphatic, and immune cell types [1]. Progesterone (P4) and estradiol (E2) production by the CL, which is dependent on pituitary-derived luteinizing hormone (LH), peaks between the mid and mid-late luteal phase. As the CL undergoes luteolysis, the steroidogenic cells become less responsive to LH and consequently P4 and E2 production declines. Blood volume and vascular flow within luteal tissue is also reduced in the late luteal phase [2] due to vascular atrophy and endothelial cell apoptosis [3]. In domestic animal species, extensive evidence exists demonstrating a critical role for endometrial-derived prostaglandin $F_{2\alpha}$ in inducing luteal regression [4]. Although limited, there is also evidence supporting a role for intraluteal $PGF_{2\alpha}$ in primate luteal regression [5]. However, the actual events that lead to the loss of luteal cell sensitivity to LH signaling, cessation of steroid biosynthetic capability, and tissue remodeling ultimately resulting in structural demise of the primate CL are still unclear.

Experimental evidence gathered from several species [6–8] including humans [9–11] implicates local actions of immune cells in the luteolytic process. Our research group recently reported $CD11b^+$ (monocytes/macrophages, neutrophils), $CD14^+$ (monocytes/macrophages), $CD16^+$ (natural killer cells; NK cells), and to a lesser extent $CD3\varepsilon^+$ (T-lymphocytes) cells all increase in rhesus macaque luteal tissue 3 days after functional regression (serum P4 $\leq$ 0.3 ng/ml), i.e. during structural regression, which is at the onset of menstruation [12]. Monocytes/macrophages, neutrophils, and T-cell numbers within the CL were at their lowest during the functional luteal phase. In contrast, the number of $CD16^+$ (NK) cells present within luteal tissue was actually comparable in functional and regressing CL [12]. At present, it is uncertain what role immune cells play in regulating luteal function and lifespan in primates.

The significant influx of immune cells that occurs after P4 synthesis ceases, particularly innate immune cells, may be important for secreting of a wide range of cytokines, chemokines, and growth factors that regulate regressive events in the luteal tissue, including tissue remodeling. Activated macrophages, neutrophils, and T-lymphocytes secrete a variety of cytokines and chemokines [6, 8, 13], many of which could contribute to induction of apoptosis in steroidogenic luteal cells [14]. In addition to coordinating cellular reorganization and tissue remodeling through locally produced cytokines/chemokines, there may be direct actions of immune cells on luteal cells. For example, expression of the cell surface receptor CD16, used to identify putative NK cells in primate luteal tissue [12], is associated with high levels of cytotoxic activity [15].

Female rhesus monkeys [16] and women [17] both have a 28-day menstrual cycle with similar circulating patterns of P4 and E2 during the luteal phase. Thus, studies of luteal function in rhesus macaques provide excellent insight into processes regulating primate CL structure and function. Several studies of the rhesus CL transcriptome by our research group noted that mRNAs associated with immune processes significantly change throughout the luteal phase of the normal menstrual cycle [18] and during luteal regression [19, 20]. In particular, several genes included in the gene ontology *Cytokine Activity* had increased mRNA levels in CL undergoing regression in the natural menstrual cycle [19]. Likewise, the levels for mRNAs encoding proteins within the Kyoto Encyclopedia of Genes and Genomes (KEGG) pathway *Molecular Mediators of Immune Responses* increased after 3 days of treatment with a gonadotropin-releasing hormone (GnRH) antagonist, which induces premature luteolysis by blocking pituitary production of luteotropic LH [20]. Finally, in a larger gene set enrichment analysis that compared the luteal transcriptome during natural regression against two separate databases of GnRH antagonist-induced luteolysis in macaque species [21], several mRNAs within the gene ontology *Immune System Processes* increased following natural and induced luteolysis. These studies provide evidence that several of the immune cell types identified within macaque CL may be producing cytokines and chemokines, which could contribute to functional and structural regression of the primate CL.

To assess our hypothesis that the numbers of immune cells and immune-associated activities increase within the nonhuman primate (NHP) CL during late regression, immune cell distribution and cytokine/chemokine production were compared between functional and late stage CL (prior to, and undergoing structural regression) of rhesus macaques during the natural menstrual cycle.

Materials and methods

All procedures were performed with luteal tissue obtained from adult, female rhesus macaques with a history of normal menstrual cycles housed at the Oregon National Primate Research Center (ONPRC). All animal protocols and procedures were approved by the Oregon Health & Science University (OHSU)/ONPRC Institutional Animal Care and Use Committee. ONPRC strictly adheres to the American Society of Primatologists Principles for the Ethical Treatment of Nonhuman Primates and the Animal Welfare Act (AWA; 1985) of the USA. Animals were under the direct care of the ONPRC Department of Comparative Medicine (DCM) and protocols requiring sterile aseptic surgical procedures were performed by surgical veterinarians and technicians in the DCM Surgical Services Unit.

Tissues for immunohistochemistry

Archived paraffin-embedded CL dissected from rhesus macaque ovaries at discrete, defined stages of the luteal phase were prepared as described previously [12, 18, 20]. Archived paraffin-embedded uteri and associated placenta from pregnant rhesus monkeys and peripheral lymphoid rhesus tissue (mesenteric lymph node and tonsil) were obtained from the ONPRC NHP Tissue Distribution Program.

Immunohistochemistry methods

All tissues were processed for immunohistochemical analyses as previously described [22]. In brief, paraffin-embedded tissue was cut into 5 μm sections that were then placed on glass permafrost slides. These sections were deparaffinized, rehydrated, and then subjected to

citrate-buffer heat-mediated antigen retrieval for 3 min. After washing the slides twice with phosphate-buffered saline (PBS)/0.025% Triton X-100 (PBST) for 5 min, sections were incubated with normal goat serum for 2 h at room temperature. Sections were then incubated with either primary antibodies that recognize the protein of interest or a nonspecific IgG control (Supplemental Table S1A and B). All sections were washed again with PBST, then incubated with PBS containing 0.3% H_2O_2 for 15 min. Finally, sections were incubated with a horseradish peroxidase-conjugated secondary antibody (either goat anti-mouse or goat anti-rabbit VECTASTAIN® Elite ABC system, Vector Laboratories, Inc. Burlingame, CA), washed with PBST, and developed using a colorimetric generating system (DAB; Thermo Fisher Scientific Inc. Waltham, MA).

Isolation of immune cell populations from luteal tissue and blood of rhesus macaques

Serum E2 levels of rhesus macaque females (n = 7) were monitored as previously described [2] to determine the midcycle peak indicative of an ovulatory LH surge. The day after E2 levels fell below 100 pg/ml was designated as the first day of the luteal phase [2]. Individual CL were collected from anesthetized females as previously described [23] during the mid-late luteal phase (days 9–12 post-LH surge, mean serum P4 = 4.5 ± 1.8 ng/ml; n = 3) and after onset of menses (CL undergoing structural regression, days 16–19 post-LH surge, P4 levels ≤ 0.3 ng/ml for 3–4 days; n = 4; termed regressing CL) [12]. Individual CL were weighed, and enzymatically dispersed by established methods [24]. Immediately prior to the surgical removal of the CL, a blood sample was obtained for isolation of peripheral blood mononuclear cells (PBMCs) by Ficoll-Paque PLUS (GE Healthcare Bio-Sciences, Pittsburgh, PA) density gradient centrifugation as previously described [25]. The dispersed cells from each CL and PBMCs were counted using a hemocytometer and assessed for viability by Trypan Blue dye exclusion (Sigma Aldrich, Saint Louis, MO).

Microbead magnetic cell separation

Two equal aliquots of cells (1.6 ± 0.3 × 10^6 cells/aliquot) from enzymatically dispersed CL and corresponding PBMCs (from mid-late (n = 3) and late (n = 4) luteal phases) were incubated with immune cell surface protein-specific antibodies validated for use in NHPs conjugated to MACS MicroBeads per manufacture's protocols for positive selection of (1) CD11b or (2) CD16 expressing cells (Supplemental Table S1C; Miltenyi Biotec Inc. [26]). MicroBead-labeled cells were passed through MACS LS Columns within the magnetic field of a QuadroMACS Separator. Flow-through was collected as the antibody-depleted fraction, and columns were removed from the field to elute the antibody-enriched fraction. These fractions were then separated into three aliquots: 2/3 were used for flow cytometric analyses to determine percentage of $CD11b^{+/}CD14^+$ or $CD16^+$ cells within fractions. The remaining aliquot was cultured to determine cytokine/chemokine production as described below.

Flow cytometric analyses of fraction composition

To verify fraction composition, aliquots of enriched and depleted fractions of dispersed CL cells and PBMCs (2/3 of isolate) were pelleted by centrifugation at 300 × g for 10 min (4°C). Aliquots were resuspended in staining buffer (FBS Staining Buffer, BD Biosciences, San Jose, CA) and analyzed separately by flow cytometry by incubation with mouse antihuman antibodies previously validated for use with rhesus macaque cells: anti-CD16, anti-CD11b, and anti-CD14 (BD Biosciences, San Jose, CA; Supplemental Table S1D) [12]. All aliquots were analyzed with a BD LSR II Flow Cytometer. Resulting histograms were analyzed using FlowJo X (version 10.0.7, Tree Star Inc.), and cell numbers were determined as the percentage of antibody-positive cells present within each aliquot.

Cytokine/chemokine Luminex assay

The remaining aliquots of antibody-enriched and depleted cell fractions (1/3 of isolate) were pelleted by centrifugation at 300 × g for 10 min (4°C) and resuspended in two equal aliquots containing either (1) RMPI-1640 media with 5% FCS (HyClone media, GE Heathcare, Inc.; control/basal) or (2) incubation media containing 1 μg/ml lipopolysaccharide (LPS; Sigma-Aldrich). Cells were incubated for 24 h at 37°C. Media were then analyzed for cytokine/chemokine production using the Monkey Cytokine Magnetic 29-Plex Luminex assay panel (Invitrogen, Thermo Fisher Scientific, Inc.). Rhesus macaque PBMCs not subjected to magnetic separation were incubated for 24 h in media with and without addition of LPS (1 μg/ml), and then media was assayed to confirm the ability of the Luminex assay system to detect stimulus-associated increases in macaque inflammatory cytokine production (Supplemental Tables S2 and S3).

Quantitative real-time PCR

Archived cDNA samples from mid-late (9–12 days post-LH surge [20]; n = 4), GnRH antagonist (Antide)-induced luteolysis ([20]; n = 4), and late stage ([12]; n = 4) rhesus monkey CL, collected as previously reported [20], were analyzed by quantitative real-time PCR (qPCR) to assess mRNA levels for the cytokine/chemokines *IL1B*, *CCL22*, *CCL2*, and *CCL3* (TaqMan Gene Expression Assays, Applied Biosystems, Thermo Fisher Scientific, Inc; Supplemental Table S4). The qPCR results were compared with an existing rhesus macaque microarray dataset [20].

Statistical analysis

All cytokine/chemokine values that fell below the limit of detection were set to zero and reported in tables as nondetectable (ND). The number of positive events recorded for immune cells, serum P4 levels, CL wet weight, real-time PCR mRNA expression, cell viability, total numbers of cells recovered from dispersed CL, and total numbers of viable cells were analyzed by generalized linear model (GLM) procedure of SAS (version 9.3; SAS Institute Inc., Cary, NC, USA). Data regarding cytokine/chemokine production from media samples was analyzed by three-way ANOVA (factors: stage, fraction, stimulation, stage by fraction, and stage by fraction by stimulation; GLM procedure of SAS). Differences between means were interrogated by least significant difference, a multiple comparison test that controls for the type I error rate.

Results

Localization of immune cell types within the macaque corpus luteum

The CL collected during mid-late luteal phase, which is prior to functional regression and loss of P4-producing capacity, contained few $CD11b^+$ (monocytes/macrophages and neutrophils) cells. The few $CD11b^+$ cells present were interspersed between large luteal cells (Figure 1A; arrow). Similarly, limited numbers of $CD68^+$ cells (monocytes/macrophages) were observed in mid-late CL (Figure 1C; arrow). Immunopositive CD16 (NK) cells were clearly evident throughout luteal tissue and mainly located near

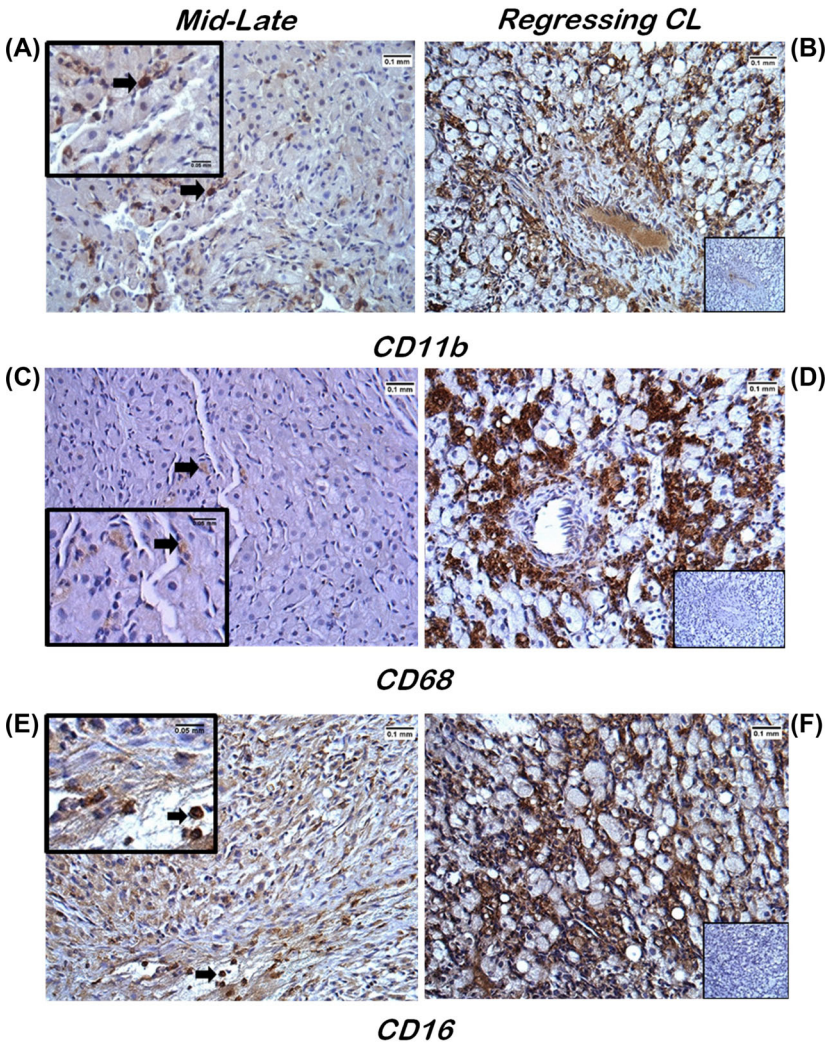

Figure 1. Immunohistochemical analyses of immune cell localization within macaque CL during the menstrual cycle. Luteal tissue sections from mid-late stage (A, C, and E) and regressing (B, D, and F) CL showed positive immunostaining (brown) for the immune cell surface proteins CD11b (monocytes/macrophages and neutrophils; A and B), CD68 (monocytes/macrophages; C and D), and CD16 (NK cells; E and F). Arrows denote individual immunopositive cells in the mid-late stage CL. Insets in panels A, C, and E are a higher magnification of the underlying panel, whereas the insets in panels B, D, and F are the IgG primary antibody staining (negative control; see Supplemental Table S1 for details). Scale bars depict widths of 0.1 and 0.05 mm in the larger images and insets, respectively.

presumptive vessels (Figure 1E; arrow). In regressing CL, after P4 synthesis reached baseline (≤0.3 ng/ml for 3–4 days), numerous $CD11b^+$, $CD68^+$, and $CD16^+$ immunostaining cells were dispersed amongst nonstaining luteal and endothelial cells (Figure 1 B, D, and F). No positive staining was detected in luteal tissue for the cell surface protein CD56 (Supplemental Figure S2A), which is reported to identify NK cells that are actively producing cytokines but possess minimal cytotoxic activity [27], although positive CD56 staining was noted in rhesus macaque uterine and placental tissues similar to previous reports (Supplemental Figure S2B) [28, 29].

Characteristics of immune cell populations of dispersed macaque corpus luteum and peripheral blood mononuclear cells

To assess the capacity of immune cell types present within functional (mid-late) and regressing luteal tissue to secrete cytokines and chemokines, single-cell suspensions were generated and cell viability as well as total numbers were assessed prior to antibody-mediated magnetic microbead cell separation. Serum P4 levels and luteal wet weights were significantly lower for regressing CL compared to those collected in the mid-late luteal phase ($P < 0.03$ and $P < 0.003$, respectively; Figure 2A and B). Fewer cells were recovered from regressing CL compared to mid-late stage CL ($P < 0.02$; Figure 2C). However, there were no differences in the percent viability of these cells recovered between mid-late and regressing dispersed CL ($P > 0.8$, overall viability of all CL 91.7 ± 5.3%; Figure 2D). There were also no significant differences in numbers of PBMCs collected from rhesus females at lutectomy by luteal stage ($P > 0.7$, $1.1 \pm 0.2 \times 10^6$ PBMCs/female).

Microbead magnetic enrichment of immune cells from macaque corpus luteum and peripheral blood mononuclear cells

Aliquots of dispersed cells isolated from mid-late CL (Figure 3A, open bars) processed with CD11b antibody-labeled MicroBeads contained 60.5 ± 6.5% $CD11b^+$ cells, compared to 1.3 ± 0.4%

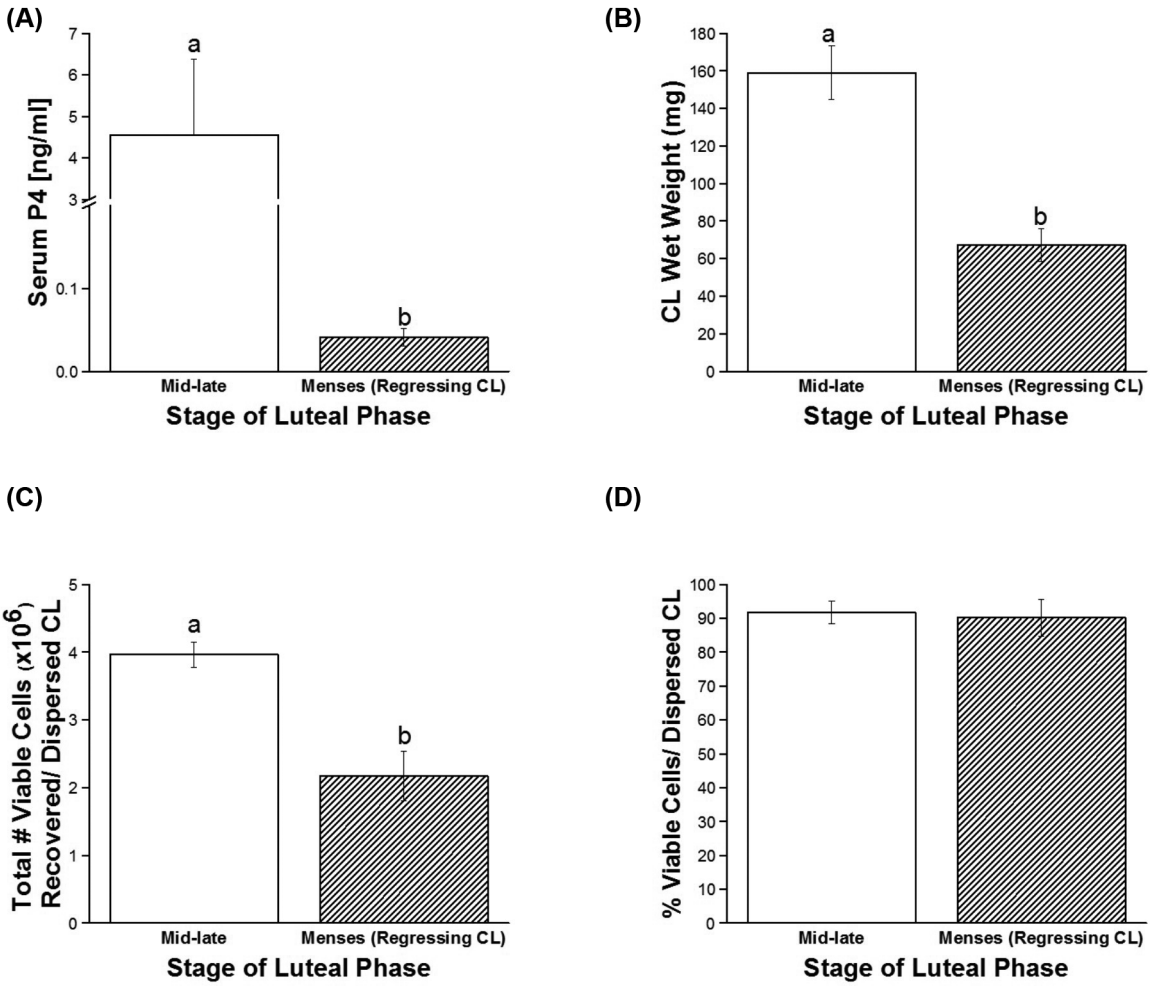

Figure 2. Characteristics of macaque CL structure and function on the day of luteal collection. Serum P4 levels (A), luteal wet weight (B), as well as total number of viable cells (C) and percent viability of cells recovered after enzymatic dispersal of CL (D) were assessed at mid-late stage and near menses (regressing CL). Different letters indicate significant differences ($P < 0.05$) by stage of the luteal phase.

remaining in the depleted column flow-through fraction ($P < 0.0001$). Within the CD11b-enriched fraction, 37.3 ± 1.5% of cells were $CD14^+$. Negligible numbers of $CD14^+$ cells were present within the CD11b-depleted fraction (0.5 ± 0.2%; Figure 3A; $P < 0.0001$). Incubation of cells dispersed from mid-late CL with CD16 antibody-conjugated microbeads enriched $CD16^+$ cells by 48.9 ± 3.2% compared to 4.6 ± 1.8% $CD16^+$ cells in the depleted fraction (Figure 3B; $P < 0.0001$). Similar results were obtained for enrichment of $CD11b^+$ and $CD16^+$ cells from PBMCs (Supplemental Figure S1A and B).

The percent enrichment for $CD11b^+$ cells in preparations isolated from regressing CL (Figure 3A, hatched bars) was comparable to those of mid-late CL. Use of CD11b microbeads increased the number of $CD11b^+$ cells by 44.5-fold (mid-late) and 23.1-fold (regressing) within the enriched population ($P < 0.001$). In addition, the percentage of $CD14^+$ cells was also enriched by 67.9-fold (mid-late) and 37.2-fold (regressing) in the CD11b-microbead selected fraction ($P < 0.0001$). However, a greater percent enrichment was detected for $CD16^+$ cells (Figure 3B) in preparations derived from mid-late CL than those from regressing CL (48.9 ± 3.2% versus 19.8 ± 7.2%); anti-CD16 microbeads enriched $CD16^+$ cells 10.7-fold (mid-late; $P < 0.0001$) and 3.5-fold (regressing; $P < 0.05$). The CD16-depleted fractions from mid-late and regressing CL were comparable in terms of the presence of $CD16^+$ cells (4.6 ± 1.8% versus 5.7 ± 3.9%, respectively).

Cytokine production by peripheral blood mononuclear cells

Media from unsorted PBMCs cultured for 24 h contained detectable concentrations of 11 out of the 29 cytokines/chemokines that can be simultaneously assayed through the Monkey Cytokine 29-Plex Luminex® panel (Supplemental Table S2. See Supplemental Table S3 for limits of assay sensitivities). Of these, four were detected under basal conditions, but levels of three increased at least 4-fold in response to LPS (Supplemental Table S2). An additional seven were only detected after LPS stimulation.

At mid-late stage of the luteal phase, $CD11b^+$ and $CD16^+$ cells enriched from PBMCs did not produce any detectable cytokines/chemokines under basal culture conditions (Table 1). However, after the onset of menses and when circulating levels of P4 dropped below 0.1 ng/ml, the CD11b-enriched PBMC fraction produced two detectable chemokines (CCL2 and CXCL8) and one lymphokine (MIF), whereas $CD16^+$ cells produced the lymphokine

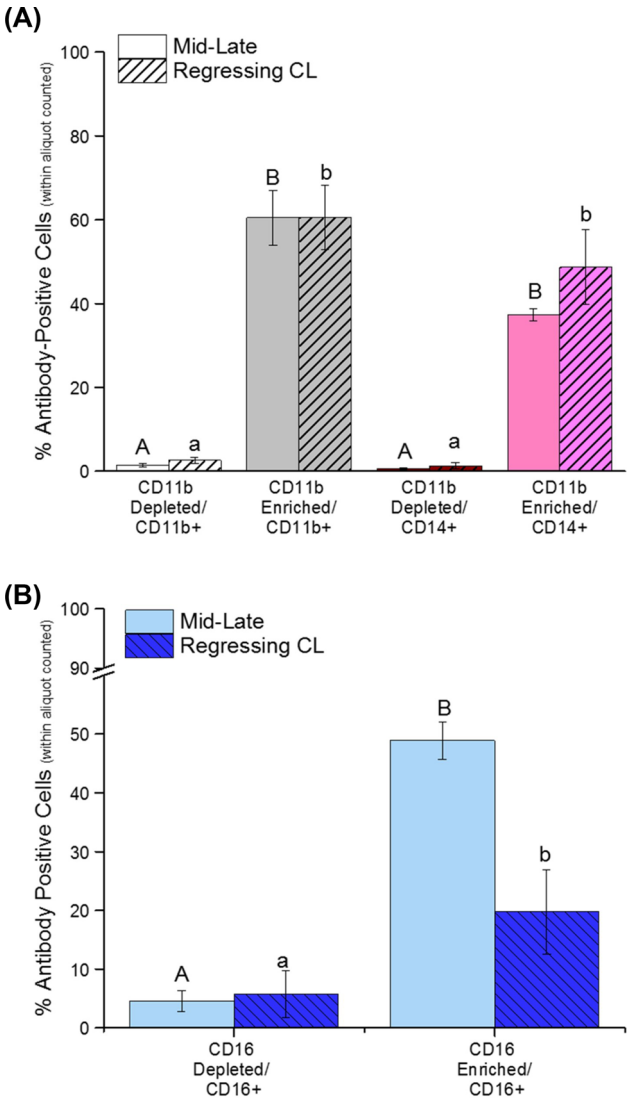

Figure 3. Flow cytometric assessment of CD11b$^+$ and CD16$^+$ cell enrichment from rhesus macaque CL. Panel A shows the percentage of CD11b$^+$ (monocyte/macrophage and neutrophil) and CD14$^+$ (monocyte/macrophage) cells within aliquots of dispersed cells obtained from mid-late stage and regressing CL. Fractions were subdivided as either the depleted/flow-through or CD11b-enriched cells (see Methods section for details). Panel B shows the percentage of CD16$^+$ cells obtained from dispersed mid-late stage and regressing CL after magnetic microbead CD16 depletion (column flow-through) or enrichment. Different letters indicate significant differences between depleted and enriched fractions ($P < 0.05$).

MIF (Table 1) in the absence of an exogenous stimulation (e.g. LPS). CD11b$^+$ PBMCs obtained at mid-late luteal phase and menses (regressing CL) produced several cytokines/chemokines only under LPS-stimulated culture conditions, while PBMC-enriched CD16$^+$ cells only responded to LPS near menses (Table 1).

Cytokine production by immune cells isolated from corpus luteum

We next analyzed the capacity of CD11b- and CD16-enriched and depleted populations of cells isolated from mid-late and regressing CL to produce cytokines in the absence of any exogenous stimulus (Table 2). Similar to PBMCs, overall basal production of detected cytokines/chemokines from all enriched fractions (CD11b and CD16) increased, both in the total number of proteins produced and in concentration, in media from cells isolated from CL after P4 production ceased (i.e. in regressing CL). In terms of CD11b$^+$-enriched cells, those from mid-late stage CL produced a total of three cytokines/chemokines: CCL2, CCL3, and CXCL8 (Table 2), all of which were not detected in PBMCs obtained at the mid-late luteal phase. In contrast, CD11b$^+$-enriched cells isolated from dispersed regressing CL produced a total of eight cytokines/chemokines, including CCL2, CCL3, CCL4, CCL22, CXCL8, IL1B, IL6, and MIF (Table 2). Of these, only CCL2, CXCL8, and MIF were produced by PMBCs isolated near menses.

Production of the chemokines CCL2, CCL3, and CXCL8 increased 7.9, 5.2, and 23.5-fold, respectively, by CD11b$^+$ -enriched cells isolated from regressing CL, compared to those of mid-late stage CL (effect of luteal stage, $P < 0.05$; see Supplemental Table S3 for assay limits of detection). Chemokine/cytokine production by cells obtained from the CD11b-depleted fraction/flow-through from mid-late and regressing CL was below the lower limit of detection of the Luminex® assay (data not shown).

Unlike enriched CD16$^+$ PBMCs obtained at mid-late luteal phase, enriched CD16$^+$ cell populations obtained from mid-late stage CL produced the chemokine CCL2 (Table 2). However, CD16-enriched cells obtained from regressing CL also produced the lymphokine MIF, similar to CD16$^+$ PBMCs. Secretion of CCL2 by CD16$^+$ cells was not significantly different between cells isolated from mid-late and regressing CL. Enriched CD16$^+$ cells produced detectable levels of CXCL8 only when collected from regressing CL (Table 2). The CD16-depleted fraction obtained from regressing CL produced IL1B, CCL3, CCL4, CCL2, CCL22, MIF, and CXCL8 at elevated levels (data not shown), similar what was observed in CD11b-enriched fractions obtained after functional luteal regression (Table 2).

Since resident immune cells in the primate CL can secrete several inflammatory cytokines, we next determined whether they have the capacity to respond to further inflammatory stimuli, i.e. following addition of LPS into culture media (Supplemental Table S5). Overall, isolated cells increased their production of CXCL8 (effect of LPS stimulation; $P < 0.04$) and CCL3 ($P < 0.0008$). In cells obtained from mid-late stage CL, LPS induced detectable levels of IL6 and CCL4 within media from the CD11b-enriched fraction, and IL6, CCL3, CCL4, and CXCL8 by CD16$^+$ cells. The CD11b-enriched cells obtained from regressing CL exposed to LPS produced detectable levels of tumor necrosis factor (TNF, commonly referred to as TNFα). Treatment of enriched CD16$^+$ cells isolated from regressing CL with LPS increased CCL3 and IL6 production (Supplemental Table S5).

Expression of cytokine/chemokine mRNA in functional and regressed rhesus macaque corpus luteum

To further assess the changes in immune cell function in the primate CL, mRNA levels for several detected cytokines/chemokines were compared between functional (mid-late) CL versus CL obtained (1) from the mid-luteal phase after treatment with 3 days of a GnRH antagonist Antide (gonadotropin depletion, induced regression) and (2) at menses in the natural menstrual cycle (regressing CL). Using real-time PCR to confirm earlier microarray analyses [19, 20], *CCL2*, *CCL3*, *CCL22,* and *IL1B* mRNA levels increased in macaque CL obtained after natural or Antide-induced regression (P4$\leq$ 0.3 for $\geq$3 days) compared to mid-late stage CL

Table 1. Cytokine production by PBMC microbead fractions: basal and LPS stimulation

	CD11b-enriched fraction				CD16-enriched fraction			
Cytokine/ chemokine/ growth factor	Mid-late stage basal	Mid-late stage + LPS	Late/menses basal	Late/menses + LPS	Mid-late stage basal	Mid-late stage + LPS	Late/menses basal	Late/menses + LPS
MCP-1/CCL2	ND	23 ± 7	20 ± 3	108 ± 56	ND	ND	ND	ND
MIP-1α/CCL3	ND	109 ± 46	**ND[a]**	**891 ± 675[b]**	ND	ND	ND	74 ± 50
MIP-1β/CCL4	ND	31 ± 4	ND	48 ± 19	ND	ND	ND	ND
MDC/CCL22	ND	405 ± 191	ND	ND	ND	ND	ND	ND
IL-8/CXCL8	ND	215 ± 103	**18 ± 10[a]**	**548 ± 359[b]**	ND	ND	ND	12 ± 5
IP-10/CXCL10	ND	ND	ND	ND	ND	ND	ND	ND
IFNγ/IFNG	ND	ND	ND	ND	ND	ND	ND	ND
IL-1β/IL1B	ND	4 ± 1	**ND[a]**	**24 ± 20[b]**	ND	ND	ND	5 ± 1
IL6	ND	107 ± 58	**ND***	**174 ± 140****	ND	ND	ND	30 ± 23
MIF	ND	ND	38 ± 26	30 ± 18	ND	ND	25 ± 16	28 ± 18
TNFα/TNF	ND	ND	ND	28 ± 11	ND	ND	ND	24 ± 6
Total number detected each fraction	***0***	***7***	***3***	***8***	***0***	***0***	***1***	***6***

Mean ± SEM(pg/ml).

ND = nondetectable; see Supplemental Table S3 for limits of detection for each assay.

Different letters indicate significant differences within marker for each cytokine by LPS stimulation; asterisks indicate trend (P = 0.08) toward difference by LPS stimulation.

Table 2. Cytokine production by luteal immune cell microbead fractions under basal culture conditions

	CD11b-enriched fraction		CD16-enriched fraction	
Cytokine/chemokine/ growth factor	Mid-late stage basal	Late/menses basal	Mid-late stage basal	Late/menses basal
MCP-1/CCL2	**122 ± 53***	**972 ± 483****	37 ± 21	20 ± 4
MIP-1α/CCL3	**30 ± 6[a]**	**156 ± 59[b]**	ND	ND
MIP-1β/CCL4	ND	48 ± 21	ND	ND
MDC/CCL22	**ND[a]**	**1073 ± 579[b]**	ND	ND
IL-8/CXCL8	21 ± 6	489 ± 247	**ND***	**8 ± 1****
IP-10/CXCL10	ND	ND	ND	ND
IFNγ/IFNG	ND	ND	ND	ND
IL-1β/IL1B	ND	6 ± 1	ND	ND
IL6	ND	23 ± 15	ND	ND
MIF	ND	40 ± 18	ND	10 ± 1
TNFα/TNF	ND	ND	ND	ND
Total number detected each fraction	***3***	***8***	***1***	***3***

Mean ± SEM(pg/ml).

ND = nondetectable; see Supplemental Table S3 for limits of detection for each assay.

Different letters indicate significant differences within marker for each cytokine between luteal stage; Asterisks indicate trend (P < 0.07) toward difference within marker between luteal stage.

(Figure 4A–D: *CCL2*, *IL1B*, $P < 0.0001$; *CCL3*, $P < 0.003$; *CCL22*, $P < 0.002$). The changes in *CCL2*, *CCL3*, *CCL22*, and *IL1B* mRNA levels are consistent with their increased secretion by dispersed cell preparations isolated from regressing CL (Table 2). Microarray and real-time PCR analyses demonstrate similar patterns of mRNA expression within samples from the same group. A 30-fold increase in *CCL22* mRNA was observed between mid-late (days 9–12 following LH surge) and regressing rhesus CL (Figure 4C; $P < 0.001$). Similarly, the highest level of CCL2 mRNA expression (Figure 4A) was detected in CL after natural and Antide-induced luteal regression. Moreover, 3-fold increases in IL1B and CCL3 mRNA expression were detected in regressing CL compared to mid-luteal stage (Figure 4B and D).

Discussion

We previously reported a large increase in cells positive for several surface proteins associated with immune cells by flow cytometry within preparations from the rhesus macaque CL during luteal regression, i.e. after P4 levels fall below 0.3 ng/ml for 3–4 days at the end of the natural menstrual cycle: CD11b (ITGAM), CD14, and CD16 (FCGR3) [12]. This study demonstrated that at the mid-late luteal stage when the CL is still functional, luteal $CD16^+$ NK cells outnumber $CD11b^+$ macrophages/monocytes/neutrophils 5 to 1. Once serum P4 levels decline to baseline (≤ 0.3 ng/ml), however, flow cytometry revealed that there are approximately even numbers of $CD16^+$ and $CD11b^+$ cells within primate luteal

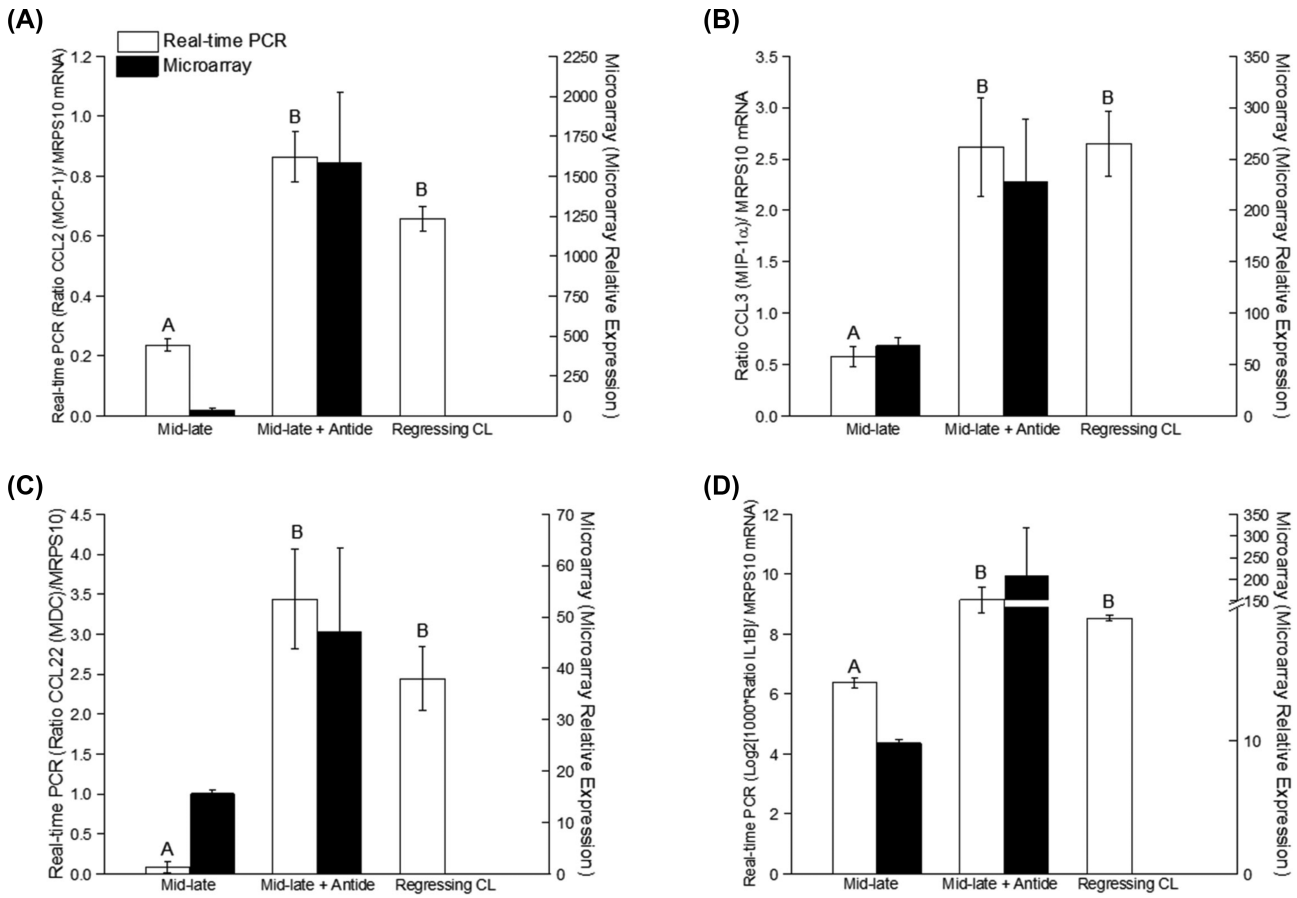

Figure 4. Levels of select cytokine/chemokine mRNAs within functional mid-late CL or in either induced (mid-late+Antide) or naturally regressing CLin vivo. The mRNA expression of *CCL2* (A), *CCL3* (B), *CCL22* (C), and *IL1B* (D) was determined by real-time PCR (open bars) and DNA microarray (black bars; previously reported [19, 20]). Different letters indicate significant differences measured by real-time PCR between groups ($P < 0.05$).

tissue [12]. We now confirm these findings and define their distribution within luteal tissue by immunohistochemistry (IHC). An antibody suitable for IHC detection of the macrophage-specific protein CD14 in paraffin-embedded macaque tissue was not identified. Rather, the monocyte/macrophage surface protein CD68 was used to confirm the flow cytometry data, demonstrating increased monocyte/macrophage numbers in the regressed CL. Moreover, the cellular morphology of specific immunostained cells within CL is consistent with neutrophils ($CD11b^+$), macrophages/monocytes ($CD11b^+$, $CD68^+$), and NK cells ($CD16^+$), but differed from the unstained luteal and vascular endothelial cell types.

Enrichment of specific immune cell populations from dispersed luteal cells was performed to assess their ability to produce cytokines and chemokines, which in turn may play a role in recruiting additional inflammatory cells and orchestrating events involved in the tissue remodeling within the regressing CL. Antibody-mediated microbead enrichment of immune cell populations was chosen over flow cytometry-based methods to prevent artificial immune cell activation or decreased cell viability [26]. We validated the ability of the microbead technique to effectively enrich rhesus macaque immune cell populations from PBMCs. Thus, using this magnetic microbead method, we achieved a 44.5-fold ($CD11b$) and 3.5-fold ($CD16$) enrichment from dispersed luteal tissue. Differences in enrichment of $CD16^+$ cells between mid-late and regressing CL were not due to loss of anti-$CD16$ microbead specificity: PBMCs processed in tandem with luteal cell preparations resulted in a 4.7- to 3.6-fold enrichment (Supplemental Figure S1B).

Our results demonstrate that the macrophages and neutrophils ($CD11b^+$ cells) present in the regressing primate CL appear to be activated based on the chemokines/cytokines that they secrete [6, 11]. Similar to results obtained from studies of other tissues [8, 13, 15], the $CD11b^+$-enriched fraction from the macaque CL produced the majority of cytokines/chemokines (Table 2) compared to relatively few produced by $CD16^+$ NK cells. $CD11b^+$ cells enriched from mid-late CL produced three chemokines: CCL3, CCL2, and CXCL8, all of which are secreted by macrophages, monocytes, and neutrophils [30, 31]. These three chemokines function to recruit additional macrophages, monocytes, and neutrophils into tissues, and could have similar functions in luteal tissue. The chemokine CXCL8 is a potent chemoattractant for neutrophils [30], and CXCL8 production by bovine luteal tissue is reported to fluctuate throughout the luteal phase [32]. Increased CXCL8 synthesis by $CD11b^+$ cells obtained at/near menses could reflect not only a response to endogenous luteolytic processes, but also correspond with increased numbers of $CD11b^+$, $CD14^+$, and other immune cell types within luteal tissue at this stage [12]. The cytokines/chemokines IL6, IL1B, MIF, and CCL4 were only produced by the $CD11b$-enriched cells obtained from regressing CL. These factors are known to induce monocyte differentiation to macrophages [33], classical macrophage activation [34], macrophage survival and function

[35], and immune cell recruitment [31]. Our findings suggest a dynamic process of immune cell recruitment (particularly neutrophils and monocytes/macrophages), macrophage activation, and sustained macrophage function within the primate CL during luteal regression. Notably, chemokine/cytokine production by CD11b$^+$ cells occurs in the absence of an acute exogenous stimulus such as LPS or prostaglandins. This is not observed in the PBMCs collected and processed at the same time, wherein only three chemokines/lymphokines are produced under basal conditions (CCL2, MIF, CXCL8; Table 1) and an additional eight are detected following LPS stimulation (Table 1). The increased number of endogenously produced chemokines/cytokines by monocytes/macrophages/neutrophils in regressing CL indicates that these immune cells are activated by an undefined mechanism in regressing luteal tissue, in the absence of a typical inflammatory stimulus. It cannot be determined from these studies if there is a per cell increase in cytokine/chemokine production or if the increased levels are due to elevated numbers of CD11b$^+$ cells present within the regressing CL relative to the mid-late stage CL, since an equivalent number of total cells were subjected to magnetic cell sorting and the number cultured were not determined afterwards. Thus, future studies are planned to determine if increased luteal CD11b$^+$ cell cytokine/chemokine-producing potential directly increases after the loss of P4 synthesis.

Several cytokines secreted by macrophages also increase the cytotoxic potential of NK cells [15]. Expression of the cell surface receptor CD16, used to identify putative NK cells in primate luteal tissue [12], is associated with higher levels of cytotoxic activity [15]. The enriched CD16$^+$ cells within the macaque CL show limited cytokine/chemokine production, which is consistent with reported functions of CD16$^+$ NK cells isolated from other tissues [15]. Typically, the CD16$^+$ subset of NK cells has a limited capacity for cytokine production, but instead functions to destroy target cells by releasing granzyme and perforin to lyse cell membranes [36]. Enzymatically dispersed CL enriched for NK (CD16$^+$) cells produced the fewest chemokines/cytokines (Table 2); only CCL2 was produced by fractions from mid-late CL, and low levels of CCL2, MIF, and CXCL8 were produced by CD16$^+$ cell fractions from CL collected at menses. The low basal production of CCL2, MIF, and CXCL8 by cells isolated from CL collected at mid-luteal phase might be due to other cell types present within this fraction, given that only 20%–40% of the cells within this fraction were identified as CD16$^+$ by flow cytometry analysis. It is important to note that production of these chemokines by the CD11b-depleted fraction was similar (data not shown), suggesting that cells other than neutrophils, macrophages, and monocytes present in the CD16-enriched fraction are producing these chemokines. Although macaque NK cells were previously reported to be predominantly CD16$^+$ [37], some NK cells also express CD56 [36]. The majority of NK cells with high levels of CD56 expression (CD56^{bright}) typically do not express CD16 (CD16$^-$) [15] and produce many cytokines that enhance vascular development of the placenta during pregnancy [36, 38]. We did not observe specific staining for CD56 in rhesus macaque ovarian/luteal tissue by IHC (Supplemental Figure S2), similar to previous studies that failed to identify CD56 expressing cells in ovarian/luteal tissue from women [9]. Thus, NK cells within the primate ovary may represent a functionally distinct subset compared to NK cells residing within the uterus. It is recognized that CD16 expression is found on other immune cell types [39], therefore, further experiments characterizing CD16$^+$ cells by flow cytometric and other functional analyses are needed to confirm that they are NK cells and to define their role within the ovary [40].

Both CCL2 and CCL22 were produced at significantly higher levels by CD11b$^+$ cells within functionally regressed CL relative to those from functional CL. In fact, CCL22 (also known as macrophage-derived chemokine, or MDC) production by CD11b$^+$ cells collected from mid-late stage CL was below the limit of detection. This chemokine is a 69-amino-acid protein in the mature secreted form and is a potent chemoattractant for monocytes and NK cells [41, 42]. Previously, ovarian macrophage production of CCL22 was mainly reported from neoplastic tissue/carcinomas [43]. The large increase in production of CCL22 by CD11b$^+$ cells within the regressing macaque CL parallels a 30-fold increase in *CCL22* mRNA. High levels of CCL22 might function to recruit NK cells to luteal tissue to facilitate luteolytic processes. The earlier rise in NK cells observed in rhesus CL between early and mid-luteal phase [12] might be associated with a rise in CCL22 production by low numbers of macrophages present at these time points and warrants further investigation. Another chemokine, CCL2, is widely implicated in luteolytic processes in many mammalian species [44], and is suggested to be one of the main drivers increasing total numbers of immune cells present within luteal tissue at onset of regression [45]. It is reported that luteal cells are a major source of CCL2 in the primate CL at the mid-late stage [45]. Therefore, nonimmune cell types might contribute to the low basal levels of CCL2 secretion into media from cells isolated at mid-luteal stage.

Perhaps surprisingly, one factor that was not detected under basal culture conditions within CD16$^+$ or CD11b$^+$-enriched cell fractions obtained from enzymatically dispersed CL was TNF. Production of detectable levels of TNF in culture media was only observed by CD11b$^+$ cells following LPS addition (Supplemental Table S5). Previous studies suggest that primate luteal tissue expresses mRNA for TNF, but the peak production of TNF mRNA is in functional late CL (days 14–16 following the LH surge), and by late regression (days 17–19 mRNA) levels decline to near baseline [46]. The late CL in this study were staged by days following a decline in P4 secretion below 0.3 ng/ml, similar to our previous study [12], and thus most were in the latter stages of regression. It is possible that basal production of TNF is higher earlier in luteolysis, as many studies suggest that this cytokine facilitates the initial decline in luteal P4 production during functional regression [8]. Conversely, endogenous production of this cytokine by the CD11b$^+$ macrophages under basal culture conditions might be lower than the detection limit of the current assay, but still biologically relevant since only 1 ng/ml of exogenous TNF is needed to observe the effects of this macrophage-derived cytokine in cell culture studies [47].

Interestingly, these data revealed that the response of rhesus PBMCs to an inflammatory stimulus varied by stage of the menstrual cycle (Table 1). The number of different cytokines/chemokines produced, or in some cases their level of synthesis, increased after LPS addition to CD11b$^+$ and CD16$^+$ PBMC fractions obtained in the late luteal phase (i.e. low P4) relative to those isolated at mid-late phase (i.e. high P4). This is similar to previous reports in women of varying immune responses during the menstrual cycle and pregnancy [48]. The PMBCs of reproductive aged women are less responsive to antigenic stimuli in the luteal phase compared to the follicular phase of the menstrual cycle [49]. Both estrogen receptor 1 (ESR1) and the classical P4 nuclear receptor (PGR) are detected in CD68-positive macrophages isolated from women [50]. At menses, after P4 levels decline, unopposed ESR1 activation might contribute to heightened PBMC response to antigenic stimuli. These data indicate that the overall cytokine-producing potential of circulating innate immune cells is depressed during the mid-late luteal phase in the NHP

menstrual cycle (time of luteal rescue by chorionic gonadotropin secreted by an implanting embryo [16]) compared to near the onset or during menstruation.

Collectively, these studies demonstrate that the relatively low numbers of monocytes/macrophages and neutrophils within functional primate CL (mid-late stage) secrete a limited inflammatory cytokine/chemokine repertoire. This may be due, in part, to an overall suppression of inflammatory responses by elevated P4 levels; our data indicate that macaque PBMC response to antigenic stimuli (e.g. LPS) is also suppressed in the mid-late stage of the menstrual cycle (Table 1). Once P4 levels decline below baseline for 3 or more days during luteal regression, increased synthesis of factors by $CD11b^+$ cells (e.g. neutrophils, macrophages) within luteal tissue may facilitate further increases in both immune cell types and cytokine/chemokine production, all of which may be necessary for the structural regression of the CL. Based on the secretion profile, one function of luteal neutrophils/macrophages after P4 levels decline is the production of significant levels of CCL22/MDC which may recruit additional NK cells to the CL. Luteal NK cells preferentially expressing the cell-surface receptor CD16 produce few, if any, cytokines/chemokines, unlike $CD56^+$ uterine NK cells. These luteal NK cells likely function by releasing granzyme and perforin to lyse target cells, contributing to further regression of primate luteal tissue at the end of the luteal life span and ultimately result in complete regression of luteal cell types within the primate ovary.

Supplementary data

Supplementary data are available at *BIOLRE* online.

Supplemental Figure S1. Flow cytometric analysis of PBMCs after antibody-conjugated magnetic microbead enrichment/depletion. (A) Analysis of percentage of $CD11b^+$ (monocyte/macrophage and neutrophil) and $CD14^+$ (monocyte/macrophage) cells within aliquots of PBMC obtained from female macaques at time of luteal collection at mid-late luteal stage and near menses (regressing CL). Fractions were subdivided as either depleted/flow through or enriched for CD11b-expressing ($CD11b^+$) cells after processing with anti-rhesus CD11b conjugated to magnetic microbeads (see Methods for details). Processing of aliquots of PBMCs obtained from both luteal stages resulted in less than 5% of $CD11b^+$ cells in depleted fractions/flow-through, and greater than 69% of $CD11b^+$ cells in the CD11b-enriched fraction ($P < 0.001$). Less than 0.8% of cells in the CD11b-depleted fraction were $CD14^+$, while the percentage of $CD14^+$ cells was greater than 50% in the CD11b-enriched fraction ($P < 0.0001$). (B) Percentage of $CD16^+$ cells within aliquots of PBMCs processed with anti-rhesus CD16 conjugated to magnetic microbeads. Aliquots of PBMCs isolated at the mid-late stage resulted in less than 13% of $CD16^+$ cells in the CD16-depleted fraction/flow-through, and approximately 45% of $CD16^+$ cells in the CD16-enriched fraction ($P < 0.0001$). Aliquots of PMBCs obtained near menses (regressing CL) revealed less than 10% of cells in the CD16-depleted fraction were $CD16^+$, but about 45% of the cells in the CD16-enriched fraction were $CD16^+$. Different letters indicate significant differences between depleted and enriched fractions ($P < 0.05$).

Supplemental Figure S2. Immunohistochemical (IHC) analyses of CD56-positive cells within macaque CL during the menstrual cycle and placental villi. Luteal tissue obtained at mid-late stage and menses (regressing CL) did not show positive immunostaining (brown color) for expression of CD56, while rhesus placental villi displayed detectable expression of CD56 (arrow example of CD56-positive cell). Negative control nonspecific IgG antibody staining of adjacent sections is provided in smaller images. All images visualized at ×40 magnification.

Acknowledgments

We thank Theodore Molskness, Ph.D. for providing logistical support at the beginning of the project. We also thank Kwok-Yuen Francis Pau, Ph.D. for his invaluable input on the Luminex assay employed here. The advice of Hans-Peter Raue, Ph.D., Mark Slifka, Ph.D., Jonah Sacha, Ph.D. and Ben Burwitz, Ph.D. in the ONPRC Division of Pathobiology & Immunology was instrumental to the success of this project.

References

1. Stouffer RL, Bishop CV, Bogan RL, Xu F, Hennebold JD. Endocrine and local control of the primate corpus luteum. *Reprod Biol* 2013; **13**:259–271.
2. Bishop CV, Molskness TA, Xu F, Belcik JT, Lindner JR, Slayden OD, Stouffer RL. Quantification of dynamic changes to blood volume and vascular flow in the primate corpus luteum during the menstrual cycle. *J Med Primatol* 2014; **43**:445–454.
3. Fraser HM, Dickson SE, Lunn SF, Wulff C, Morris KD, Carroll VA, Bicknell R. Suppression of luteal angiogenesis in the primate after neutralization of vascular endothelial growth factor. *Endocrinology* 2000; **141**:995–1000.
4. Lee J, McCracken JA, Banu SK, Rodriguez R, Nithy TK, Arosh JA. Transport of prostaglandin F(2alpha) pulses from the uterus to the ovary at the time of luteolysis in ruminants is regulated by prostaglandin transporter-mediated mechanisms. *Endocrinology* 2010; **151**:3326–3335.
5. Bogan RL, Murphy MJ, Stouffer RL, Hennebold JD. Prostaglandin synthesis, metabolism, and signaling potential in the rhesus macaque corpus luteum throughout the luteal phase of the menstrual cycle. *Endocrinology* 2008; **149**:5861–5871.
6. Walusimbi SS, Pate JL. Physiology and Endocrinology Symposium: role of immune cells in the corpus luteum. *J Anim Sci* 2013; **91**:1650–1659.
7. Komatsu K, Manabe N, Kiso M, Shimabe M, Miyamoto H. Changes in localization of immune cells and cytokines in corpora lutea during luteolysis in murine ovaries. *J Exp Zool A Comp Exp Biol* 2003; **296**:152–159.
8. Wu R, Van der Hoek KH, Ryan NK, Norman RJ, Robker RL. Macrophage contributions to ovarian function. *Hum Reprod Update* 2004; **10**:119–133.
9. Best CL, Pudney J, Welch WR, Burger N, Hill JA. Localization and characterization of white blood cell populations within the human ovary throughout the menstrual cycle and menopause. *Hum Reprod* 1996; **11**:790–797.
10. Brannstrom M, Pascoe V, Norman RJ, McClure N. Localization of leukocyte subsets in the follicle wall and in the corpus luteum throughout the human menstrual cycle. *Fertil Steril* 1994; **61**:488–495.
11. Castro A, Castro O, Troncoso JL, Kohen P, Simon C, Vega M, Devoto L. Luteal leukocytes are modulators of the steroidogenic process of human mid-luteal cells. *Hum Reprod* 1998; **13**:1584–1589.
12. Bishop CV, Xu F, Molskness TA, Stouffer RL, Hennebold JD. Dynamics of immune cell types within the macaque corpus luteum during the menstrual cycle: Role of progesterone. *Biol Reprod* 2015; **93**:112.
13. Futosi K, Fodor S, Mocsai A. Reprint of Neutrophil cell surface receptors and their intracellular signal transduction pathways. *Int Immunopharmacol* 2013; **17**:1185–1197.
14. Smolikova K, Mlynarcikova A, Scsukova S. Role of interleukins in the regulation of ovarian functions. *Endocr Regul* 2012; **46**:237–253.
15. Cooper MA, Fehniger TA, Caligiuri MA. The biology of human natural killer-cell subsets. *Trends Immunol* 2001; **22**:633–640.
16. Atkinson LE, Hotchkiss J, Fritz GR, Surve AH, Neill JD, Knobil E. Circulating levels of steroids and chorionic gonadotropin during pregnancy

in the rhesus monkey, with special attention to the rescue of the corpus luteum in early pregnancy. *Biol Reprod* 1975; **12**:335–345.
17. Sherman BM, Korenman SG. Measurement of serum LH, FSH, estradiol and progesterone in disorders of the human menstrual cycle: the inadequate luteal phase. *J Clin Endocrinol Metab* 1974; **39**:145–149.
18. Bogan RL, Murphy MJ, Stouffer RL, Hennebold JD. Systematic determination of differential gene expression in the primate corpus luteum during the luteal phase of the menstrual cycle. *Mol Endocrinol* 2008; **22**:1260–1273.
19. Bogan RL, Murphy MJ, Hennebold JD. Dynamic changes in gene expression that occur during the period of spontaneous functional regression in the rhesus macaque corpus luteum. *Endocrinology* 2009; **150**:1521–1529.
20. Bishop CV, Hennebold JD, Stouffer RL. The effects of luteinizing hormone ablation/replacement versus steroid ablation/replacement on gene expression in the primate corpus luteum. *Mol Hum Reprod* 2009; **15**: 181–193.
21. Bishop CV, Bogan RL, Hennebold JD, Stouffer RL. Analysis of microarray data from the macaque corpus luteum; the search for common themes in primate luteal regression. *Mol Hum Reprod* 2011; **17**:143–151.
22. Wright JW, Jurevic L, Stouffer RL. Dynamics of the primate ovarian surface epithelium during the ovulatory menstrual cycle. *Hum Reprod* 2011; **26**:1408–1421.
23. Duffy DM, Chaffin CL, Stouffer RL. Expression of estrogen receptor alpha and beta in the rhesus monkey corpus luteum during the menstrual cycle: regulation by luteinizing hormone and progesterone. *Endocrinology* 2000; **141**:1711–1717.
24. Brannian JD, Stouffer RL. Progesterone production by monkey luteal cell subpopulations at different stages of the menstrual cycle: changes in agonist responsiveness. *Biol Reprod* 1991; **44**:141–149.
25. Fuss IJ, Kanof ME, Smith PD, Zola H. Isolation of whole mononuclear cells from peripheral blood and cord blood. *Curr Protoc Immunol* 2009. 85:I:7.1:7.1.1–7.1.8. doi: 10.1002/0471142735.im0701s85.
26. Freeman BE, Hammarlund E, Raue HP, Slifka MK. Regulation of innate CD8+ T-cell activation mediated by cytokines. *Proc Natl Acad Sci USA* 2012; **109**:9971–9976.
27. Poli A, Michel T, Theresine M, Andres E, Hentges F, Zimmer J. CD56bright natural killer (NK) cells: an important NK cell subset. *Immunology* 2009; **126**:458–465.
28. Co EC, Gormley M, Kapidzic M, Rosen DB, Scott MA, Stolp HA, McMaster M, Lanier LL, Barcena A, Fisher SJ. Maternal decidual macrophages inhibit NK cell killing of invasive cytotrophoblasts during human pregnancy. *Biol Reprod* 2013; **88**:155.
29. Slukvin II, Breburda EE, Golos TG. Dynamic changes in primate endometrial leukocyte populations: differential distribution of macrophages and natural killer cells at the rhesus monkey implantation site and in early pregnancy. *Placenta* 2004; **25**:297–307.
30. Leonard EJ, Yoshimura T. Human monocyte chemoattractant protein-1 (MCP-1). *Immunol Today* 1990; **11**:97–101.
31. Schall TJ, Bacon K, Camp RD, Kaspari JW, Goeddel DV. Human macrophage inflammatory protein alpha (MIP-1 alpha) and MIP-1 beta chemokines attract distinct populations of lymphocytes. *J Exp Med* 1993; **177**:1821–1826.
32. Jiemtaweeboon S, Shirasuna K, Nitta A, Kobayashi A, Schuberth H-J, Shimizu T, Miyamoto A. Evidence that polymorphonuclear neutrophils infiltrate into the developing corpus luteum and promote angiogenesis with interleukin-8 in the cow. *Reprod Biol Endocrinol* 2011; **9**:79.
33. Chomarat P, Banchereau J, Davoust J, Palucka AK. IL-6 switches the differentiation of monocytes from dendritic cells to macrophages. *Nat Immunol* 2000; **1**:510–514.
34. Zhu L, Zhao Q, Yang T, Ding W, Zhao Y. Cellular metabolism and macrophage functional polarization. *Int Rev Immunol* 2015; **34**:82–100.
35. Roger T, David J, Glauser MP, Calandra T. MIF regulates innate immune responses through modulation of Toll-like receptor 4. *Nature* 2001; **414**:920–924.
36. Moretta A, Bottino C, Vitale M, Pende D, Cantoni C, Mingari MC, Biassoni R, Moretta L. Activating receptors and coreceptors involved in human natural killer cell-mediated cytolysis. *Annu Rev Immunol* 2001; **19**:197–223.
37. Choi EI, Wang R, Peterson L, Letvin NL, Reimann KA. Use of an anti-CD16 antibody for in vivo depletion of natural killer cells in rhesus macaques. *Immunology* 2008; **124**:215–222.
38. Tessier DR, Yockell-Lelievre J, Gruslin A. Uterine spiral artery remodeling: The role of uterine natural killer cells and extravillous trophoblasts in normal and high-risk human pregnancies. *Am J Reprod Immunol* 2015; **74**:1–11.
39. Butcher SK, Chahal H, Nayak L, Sinclair A, Henriquez NV, Sapey E, O'Mahony D, Lord JM. Senescence in innate immune responses: reduced neutrophil phagocytic capacity and CD16 expression in elderly humans. *J Leukoc Biol* 2001; **70**:881–886.
40. Weisgrau KL, Ries M, Pomplun N, Evans DT, Rakasz EG. OMIP-035: Functional analysis of natural killer cell subsets in macaques. *Cytometry A* 2016; **89**:799–802.
41. Mantovani A, Gray PA, Van Damme J, Sozzani S. Macrophage-derived chemokine (MDC). *J Leukoc Biol* 2000; **68**:400–404.
42. Godiska R, Chantry D, Raport CJ, Sozzani S, Allavena P, Leviten D, Mantovani A, Gray PW. Human macrophage-derived chemokine (MDC), a novel chemoattractant for monocytes, monocyte-derived dendritic cells, and natural killer cells. *J Exp Med* 1997; **185**:1595–1604.
43. Sica A, Schioppa T, Mantovani A, Allavena P. Tumour-associated macrophages are a distinct M2 polarised population promoting tumour progression: potential targets of anti-cancer therapy. *Eur J Cancer* 2006; **42**:717–727.
44. Penny LA. Monocyte chemoattractant protein 1 in luteolysis. *Rev Reprod* 2000; **5**:63–66.
45. Nio-Kobayashi J, Kudo M, Sakuragi N, Kimura S, Iwanaga T, Duncan WC. Regulated CC motif ligand 2 (CCL2) in luteal cells contributes to macrophage infiltration into the human corpus luteum during luteolysis. *Mol Hum Reprod* 2015; **21**:645–654.
46. Peluffo MC, Young KA, Hennebold JD, Stouffer RL. Expression and regulation of tumor necrosis factor (TNF) and TNF-receptor family members in the macaque corpus luteum during the menstrual cycle. *Mol Reprod Dev* 2009; **76**:367–378.
47. Matsubara H, Ikuta K, Ozaki Y, Suzuki Y, Suzuki N, Sato T, Suzumori K. Gonadotropins and cytokines affect luteal function through control of apoptosis in human luteinized granulosa cells. *J Clin Endocrinol Metab* 2000; **85**:1620–1626.
48. Bouman A, Heineman MJ, Faas MM. Sex hormones and the immune response in humans. *Hum Reprod Update* 2005; **11**:411–423.
49. Priyanka HP, Sharma U, Gopinath S, Sharma V, Hima L, ThyagaRajan S. Menstrual cycle and reproductive aging alters immune reactivity, NGF expression, antioxidant enzyme activities, and intracellular signaling pathways in the peripheral blood mononuclear cells of healthy women. *Brain Behav Immun* 2013; **32**:131–143.
50. Khan KN, Masuzaki H, Fujishita A, Kitajima M, Sekine I, Matsuyama T, Ishimaru T. Estrogen and progesterone receptor expression in macrophages and regulation of hepatocyte growth factor by ovarian steroids in women with endometriosis. *Hum Reprod* 2005; **20**: 2004–2013.